Research Article

Yuan Chang, Shukun Yu*, Miao Zhang, Xiuyun Zhu, Tianshu Jiang, Yuan Liu

N6-Methyladenosine-related alternative splicing events play a role in bladder cancer

https://doi.org/10.1515/biol-2022-0479
received November 28, 2021; accepted July 17, 2022

Abstract: This study investigated the role of *N*6-methyladenosine (m6A) and alternative splicing (AS) in bladder cancer (BLCA). The BLCA-related RNA expression profiles and AS events were downloaded from the UCSC Xena and SpliceSeq databases, respectively. Differentially expressed AS (DEAS) was screened, and prognostic-related DEAS events were used to construct prognostic risk models based on Cox proportional hazards regression analysis. Receiver operating characteristic curves and multivariate Cox analysis were used to evaluate the predictive efficiency and independence of these models. We also constructed a protein-to-protein interaction (PPI) network and a regulation network of splicing factors (SFs) and DEAS events. In total, 225 m6A-related prognostic-related DEAS events were identified. The predictive ability of each prognostic model was good, and the alternate terminator model showed the best performance when the area under the curve was 0.793. The risk score of the model was an independent prognostic factor for BLCA. The PPI network revealed that AKT serine/threonine kinase 1, serine- and arginine-rich SF6, and serine- and arginine-rich SF2 had higher-node degrees. A complex regulator correlation was shown in the SF and DEAS networks. This study provides insights for the subsequent understanding of the role of AS events in BLCA.

Keywords: bladder cancer, *N*6-methyladenosine, alternative splicing, enrichment analysis, splicing factor, independent prognostic factor

1 Introduction

Bladder cancer (BLCA) is a disease where a malignant tumor develops in the mucous membrane of the bladder and is a common malignant tumor in the urinary system. The etiology of BLCA is complicated and includes both external environmental and internal genetic factors [1]. The Bacillus Calmette–Guérin vaccine is mainly used to treat and prevent recurrence after transurethral resection of bladder tumors. Patients who do not respond to the drug require additional treatments. Advances in genetic understanding of BLCA and immunotherapy have led to new treatments [2,3].

Like many diseases involving tumors, BLCA can inactivate cytotoxic T cells by downregulating tumor antigen expression. Similarly, the immune system can be avoided by updating immune checkpoints and maintaining the immune environment [4]. Many immune-based biomarkers are being studied for the development of BLCA biomarkers. These studies include predictive biomarkers for patient selection, pharmacodynamic markers of target engagement, and identification and standardization of surrogate markers/endpoints to develop immunotherapy [5].

*N*6-Methyladenosine (m6A) is the most common form of RNA modification, and its regulatory factors are involved in the development of many cancers [6]. The level of modification of transcript m6A is regulated by "writers," "readers," and "erasers" [7]. Methyltransferases are known as "writers" and include KIAA1429, methyltransferase 3, *N*6-adenosine-methyltransferase complex catalytic subunit (METTL3), methyltransferase 14, *N*6-adenosine-methyltransferase subunit (METTL14), RNA-binding motif protein 15 (RBM15), WT1-associated protein (WTAP), and zinc finger CCCH-type containing 13 (ZC3H13). Its main function is to add a methyl group to the nitrogen of the sixth carbon of the aromatic ring of an adenosine residue [8]. "Reader" m6A-binding proteins mainly include heterogeneous nuclear ribonucleoprotein C (HNRNPC), YTH domain containing 1 (YTHDC1), YTH domain containing 2 (YTHDC2), YTH m6A RNA-binding protein 1 (YTHDF1), and YTH m6A RNA-binding

* **Corresponding author: Shukun Yu,** Department of Nursing, Affiliated Hospital of Beihua University, No. 12 Jiefangzhong Road, Chuanying District, Jilin, Jilin Province, 132011, China, tel: +86-0432-62166327, e-mail: yushukun0602@163.com
Yuan Chang: Department of Nursing, Affiliated Hospital of Beihua University, No. 12 Jiefangzhong Road, Chuanying District, Jilin, Jilin Province, 132011, China
Miao Zhang, Xiuyun Zhu, Tianshu Jiang, Yuan Liu: Department of Nursing, College of Nursing, Beihua University, Jilin, 132013, China

protein 2 (YTHDF2). It preferentially binds to RNA and regulates downstream functions [9]. Demethylase, an "eraser," specifically targets RNA m6A, mainly AlkB homolog 5, RNA demethylase (ALKBH5), and FTO alpha-ketoglutarate-dependent dioxygenase (FTO) [10]. Dysregulation of m6A regulatory factors leads to reduced cell proliferation, loss of self-renewal ability, developmental defects, and cell death [11]. Recently, some scholars have started studying the relationship between m6A RNA methylation regulators and BLCA. Han et al. reported that METTL3 promotes bladder tumor proliferation in an m6A-dependent manner by accelerating pri-miR221/222 [12]. Ying et al. reported that BLAC development could be promoted by m6A modification of CUB domain containing protein 1 mRNA [13].

Alternative splicing (AS) refers to the production of multiple types of mRNA from a single gene and is an important mechanism of post-transcriptional regulation. AS affects the normal growth and development of the human body and plays an important role in the occurrence and development of many diseases, including cancer. Studies have found that the loss of wild-type periostin by downregulation or AS, which produces Variant I, is closely correlated with the development of BLCA [14]. A study also found that splicing mutations were more common in both BLCA and normal bladder tissues [15].

However, it is still unclear how m6A methylation-related AS affects BLCA. In this study, we investigated how AS events related to BLCA prognosis and m6A methylation play a role in BLCA to provide new possible targets for future treatment and intervention of BLCA. A flow chart of the overall study design is shown in Figure 1.

2 Materials and methods

2.1 Data collection

The cohort gene expression RNAseq-RSEM transcripts per million of BLCA was downloaded from The Cancer Genome Atlas (TCGA) database, and 407 BLCA samples were obtained (https://portal.gdc.cancer.gov/projects/TCGA-BLCA). The Genotype-Tissue Expression database was used to download the normal bladder samples' information, and 28 normal bladder samples were obtained (https://www.gtexportal.org).

The specific percentage spliced in (PSI) value for the AS event of TCGA-BLCA was downloaded from the SpliceSeq database (http://projects.insilico.us.com/TCGASpliceSeq/) [16]. To generate as reliable a set of AS events as possible, we implemented a series of stringent filters (percentage of samples with PSI value ≥75, average PSI value ≥0.05). A total of 418 samples were obtained, including 19 normal and 405 tumor samples.

2.2 Differential expression analysis

The seven AS events were alternate acceptors (AA), alternate donors (AD), exon skipping (ES), retained intron (RI), alternate promoters (AP), alternate terminators (AT), and mutually exclusive exons (ME). Each AS event detected by the PSI value in BLCA vs. normal tissue was identified and counted using the software R-3.4.3. The corresponding p values were obtained using the t-test in the generalized linear model, and the difference multiplication relations were calculated to screen the AS with significant differences. Finally, an adjusted p value of <0.05 was set as a criterion to screen the significantly differentially expressed AS (DEAS).

2.3 Screening of m6A methylation-related DEAS

The expression of m6A methylation regulators [*METTL3*, *METTL14*, *METTL15*, *WTAP*, *RBM15*, RNA-binding motif protein 15B, *KIAA1429*, *ZC3H13*, *FTO*, *ALKBH5*, RNA-binding motif protein X-linked, *YTHDC1*, *YTHDC2*, insulin-like growth factor 2 mRNA-binding protein 1, insulin-like growth factor 2 mRNA-binding protein 2, insulin-like growth factor 2 mRNA-binding protein 3, *YTHDF1*, *YTHDF2*, YTH m6A RNA-binding protein 3, heterogeneous nuclear ribonucleoprotein a2/b1 (*HNRNPA2B1*), and *HNRNPC*] was extracted from the BLCA samples from TCGA. The Pearson correlation coefficient between the expression levels of the DEAS-corresponding genes and the expression levels of the m6A methylation regulators was calculated, and $p < 0.05$ and $|r| > 0.5$ were set as the threshold to identify the m6A methylation-related DEAS.

In addition, we analyzed the correlation between PSI of AS events and the expression levels of m6A methylation regulators.

2.4 Prognostic analysis of m6A methylation-related DEAS

The prognosis information of BLCA, including overall survival (OS) and OS status, was downloaded from TCGA

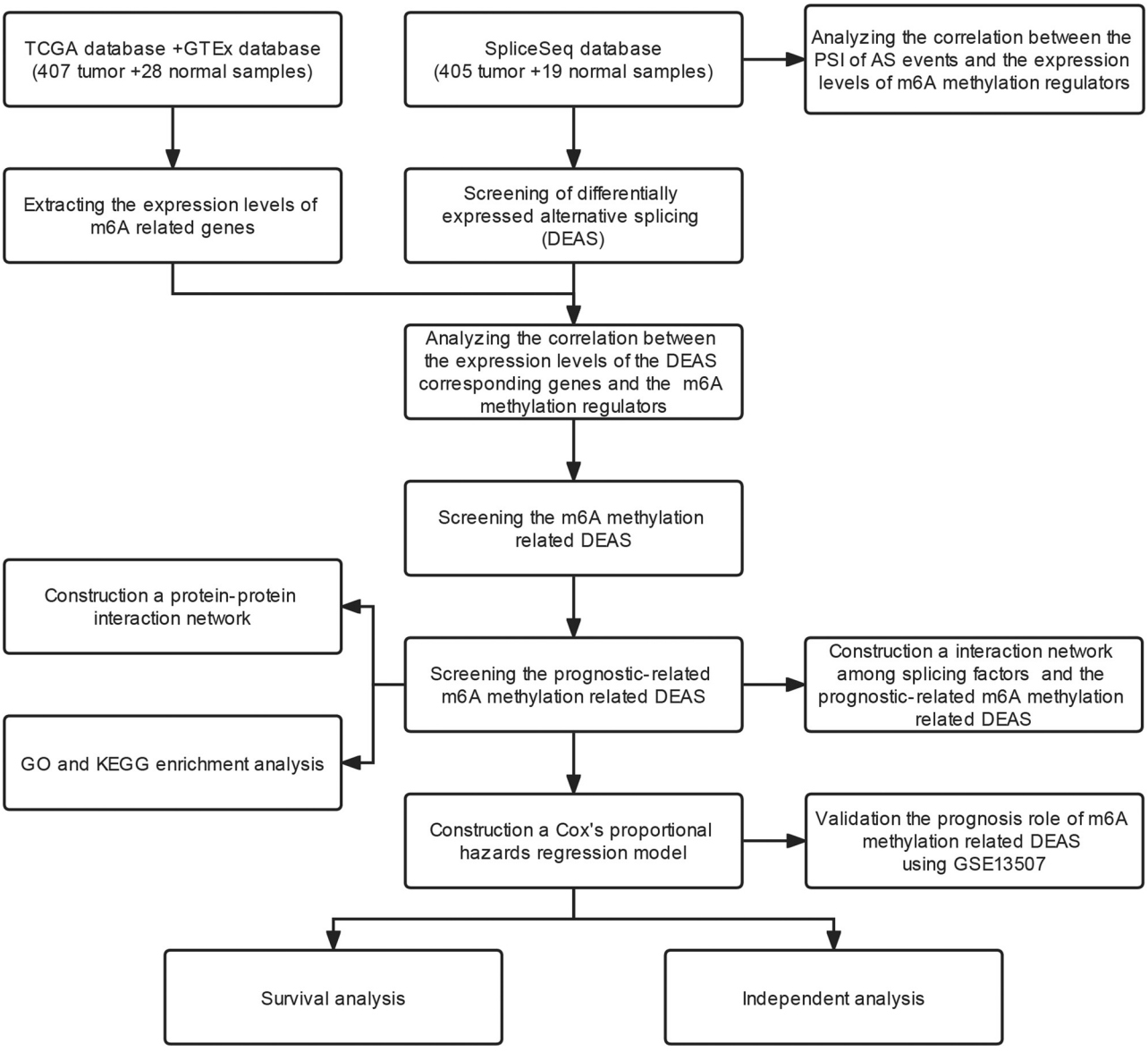

Figure 1: Research flow chart.

database. Prognostic-related m6A methylation-related DEAS was screened using univariate Cox hazard analysis in the survival package (version 2.41-1, http://bioconductor.org/packages/survivalr/) of R3.6.1. Statistical significance was set at $p < 0.05$.

2.5 Functional enrichment and pathway analysis of differentially expressed genes

The prognostic-related m6A methylation-related DEAS in the same AS type was used to perform Gene Ontology biological process (GO BP) [17] and Kyoto Encyclopedia of Genes and Genomes (KEGG) [18] enrichment analysis using clusterProfiler [19]. The significance threshold of the hypergeometric test $p < 0.01$ was set as the significant enrichment result.

2.6 Protein-to-protein interaction (PPI) network and module mining analysis

The interaction between proteins was analyzed using the STRING database (Version: 11.0, http://www.string-db.org/) [20]. The PPI score was set to 0.4. The network was then

constructed using Cytoscape (version 3.6.1) software [21] after the PPI edges were obtained.

2.7 Relationship between splicing factors (SFs) and the prognostic-related m6A methylation-related DEAS

To study the relationship between SFs and prognostic-related m6A methylation-related DEAS, we obtained 71 SFs through a literature search [22]. Subsequently, survival analysis was performed on the genes corresponding to the SFs to determine prognosis-related SFs. Pearson's test was used to assess the correlation between the expression levels of SFs and PSI of AS. $p < 0.05$ and $|r| > 0.3$ were set as the significant threshold.

2.8 Construction of Cox proportional hazards regression model

Based on the different AS types, prognostic-related m6A methylation-related DEAS was used to conduct multivariate Cox proportional hazards regression survival analysis and construct risk models. The Cox regression coefficients and PSI for each DEAS were then obtained.

$$\text{Risk score} = \sum \text{Coef AS} \times \text{Exp AS},$$

Coef AS represents the Cox regression coefficient, and Exp AS represents the PSI.

2.9 Survival analysis

The patients were divided into high-risk and low-risk groups based on their risk scores. Kaplan–Meier survival curves were constructed to compare whether there was a significant difference in prognosis between patients in the high- and low-risk groups. The survival receiver operating characteristic curve (ROC) package was used to perform an ROC analysis of these risk models.

2.10 Validation of the role of m6A methylation-related DEAS in BLCA prognosis

The GSE13507 BLCA dataset obtained from the GPL6102 Illumina human-6 v2.0 expression BeadChip sequencing platform was downloaded from the NCBI GEO (https://www.ncbi.nlm.nih.gov/) database on May 23, 2022. After excluding samples with missing survival information, 165 samples were retained for validation analysis.

2.11 Independent analysis

Univariate and multivariate Cox regression analyses were used to assess whether clinical characteristics (TNM stage, age, and sex) and risk score were independent prognostic factors for BLCA. Log-rank $p < 0.05$ was set as the threshold for screening significantly independent prognostic factors.

3 Results

3.1 AS event statistics and differential analysis

The seven types of AS patterns are shown in Figure 2a. Furthermore, we counted the number of occurrences of each AS type and the number of corresponding genes. As shown in Figure 2b, there were 2,237, 2,278, 1,900, 2,769, 3,558, 9,547, and 39 events for AA, RI, AD, AP, AT, ES, and ME, respectively. There were 1,840, 1,616, 1,549, 2,769, 3,558, 5,332, and 39 genes for AA, RI, AD, AP, AT, ES, and ME events, respectively. ES was the most frequent event among the seven AS types, whereas ME was the least frequent. We also identified 3,715 DEAS, including 1,226 downregulated and 2,489 upregulated DEAS. These 3,715 DEAS corresponded to 2,766 genes (Table S1).

3.2 Screening of prognostic-related DEAS

A total of 1,310 m6A methylation-related DEAS were identified, corresponding to 1,015 genes (Table S2). After the univariate Cox hazard analysis, six AS types were significantly associated with OS ($p < 0.05$). There were 13, 6, 38, 52, 57, and 59 AS events in AA, AD, AP, AT, ES, and RI significantly related to OS, respectively (Table S3, $p < 0.05$).We then calculated the Pearson correlation coefficients between m6A methylation regulators and AS events. As shown in Figure 2c, there was a strong correlation between m6A methylation regulators and AS events (Table S4).

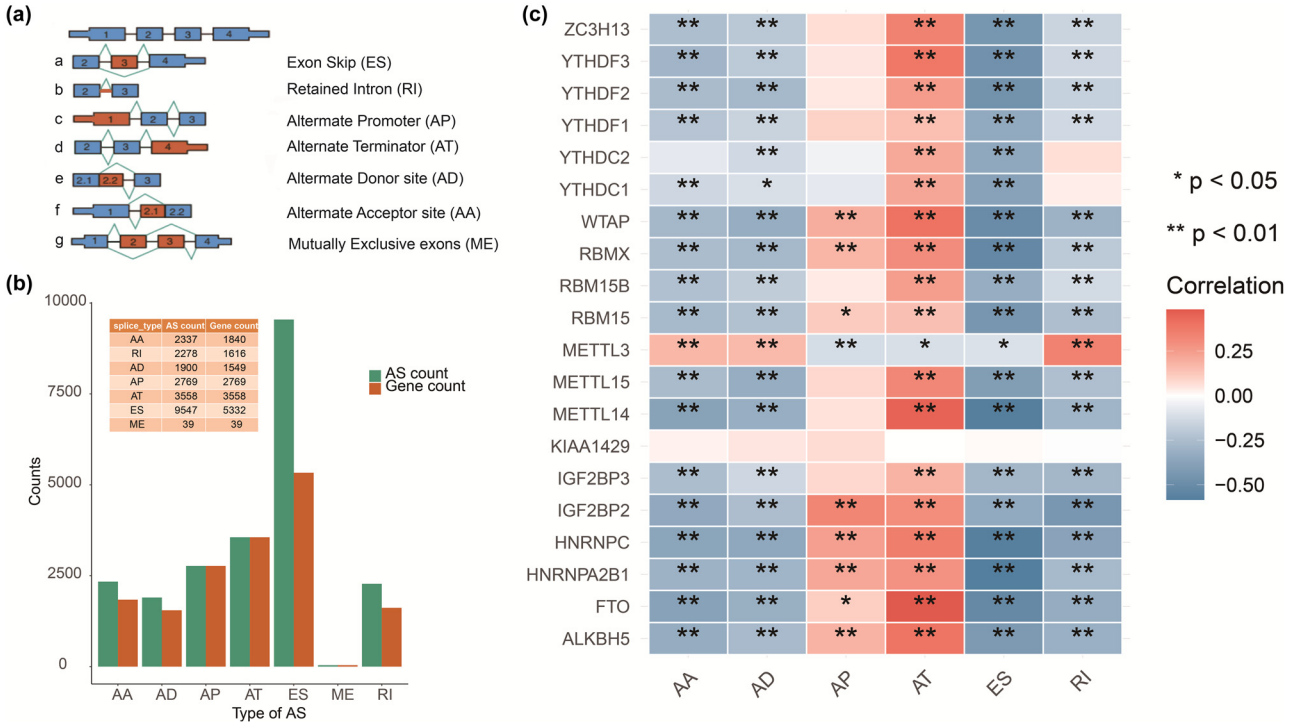

Figure 2: Different AS. (a) Schematic representation of AS events, AA and AD sites, AP, AT, ES, RI, and ME. (b) Numbers of AS events and corresponding genes in enrolled cases. (c) Correlation between m6A methylation regulators and AS events.

3.3 Function and pathway enrichment analysis of prognostic-related DEAS

The genes corresponding to the RI event were enriched in 4 KEGG and 210 GO BP pathways. These terms included spliceosome, regulation of RNA splicing, Golgi to plasma membrane protein transport, sister chromatid segregation, regulation of mRNA splicing via spliceosome, and mitochondrial calcium ion transmembrane transport (Figure S1a and b). A total of 3 KEGG pathways and 152 terms were obtained from the AT enrichment analysis. These terms were mainly involved in base excision repair and the regulation of the G2/M cell cycle phase (Figure S2a and b). The genes corresponding to AA were mainly involved in the MAPK signaling pathway, VEGF signaling pathway, and histone acetylation (Figure S3a and b). The genes corresponding to AP were mainly involved in endocrine resistance and responses to prostaglandins (Figure S4a and b). A total of 6 KEGG pathways and 174 terms were obtained from the ES enrichment analysis. These terms were mainly involved in mitotic centrosome separation, cytokinesis, and centrosome separation (Figure S5a and b). As shown in Figure S6a and b, genes in AD were mainly involved in the phospholipase D signaling pathway, antigen processing, and antigen presentation by MHC II.

3.4 The correlation network among genes in different AS events

The constructed PPI network included 110 edges and 81 nodes (Table S5 and Figure 3). The ten genes with the highest degrees in the network were Akt serine/threonine kinase 1 (*AKT1*), serine- and arginine-rich splicing factor 6 (*SRSF6*), serine- and arginine-rich splicing factor 2 (*SRSF2*), heterogeneous nuclear ribonucleoprotein a1 (*HNRNPA1*), nucleoporin 62 (*NUP62*), *HNRNPA2B1*, serine- and arginine-rich splicing factor 7 (*SRSF7*), minichromosome maintenance complex component 7 (*MCM7*), heterogeneous nuclear ribonucleoprotein l (*HNRNPL*), and heterogeneous nuclear ribonucleoprotein D like (*HNRNPDL*). Their respective cutting events were AP, ES, RI, ES, RI, AA, RI, AP, ES, and ES (Table 1).

3.5 Network of SFs and the prognostic-related DEAS

A total of eight SFs related to prognosis were obtained. These were NOVA AS regulator 1 (NOVA1), heterogeneous nuclear ribonucleoprotein H1 (HNRNPH1), QKI, KH domain

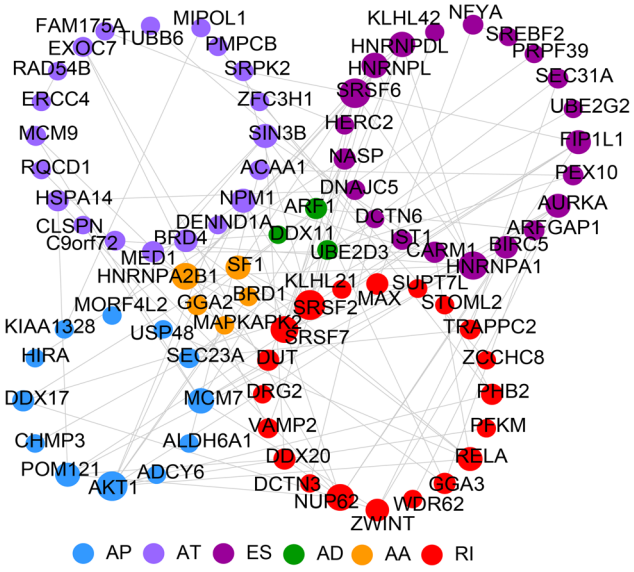

Figure 3: PPI network of prognostic-related m6A methylation-related DEAS. The blue, lavender, purple, green, yellow, and red nodes represent genes where AP, AT, ES, AD, AA, and RI have occurred, respectively. AA and AD sites, AP, AT, ES, RI. The larger the nodes, the more proteins interact with them.

containing RNA binding (QKI), splicing factor 3b subunit 1 (SF3B1), NOVA AS regulator 2 (NOVA2), TIA1 cytotoxic granule-associated RNA-binding protein (TIA1), ELAV-like RNA-binding protein 3 (ELAVL3), and RNA-binding Fox-1 homolog 2 (RBFOX2). Furthermore, we divided the patients into high- and low-expression groups according to the expression values of these eight SFs. A Kaplan–Meier (KM) curve was used to measure the difference in OS between the groups (Figure 4). Patients with low expression levels of NOVA1, NOVA2, and QKI had a better prognosis than those with high expression levels ($p < 0.05$) (Figure 4a–c). Low expression of ITA1, ELAV3, HNRNPH1, and SF3B1 was correlated with a significantly worse prognosis ($p < 0.05$) (Figure 4d–g). There was no significant difference between the prognosis of patients in the RBFOX2 high- and low-expression groups ($p = 0.05$) (Figure 4h).

The relationship between SFs expression and the PSI of AS events was analyzed. A regulatory network was constructed based on this relationship (Figure 5). This regulatory network contained 32 genes that corresponded to 34 AS events and 4 SFs (QK1, RBFOX2, TIA1, and HNRNPH1) (Table S6).

3.6 Cox proportional hazards regression model

Six Cox proportional hazards regression models were constructed using the above six OS-related AS types (AA, AD, AP, AT, ES, and RI). Patients were divided into two groups based on the risk scores calculated in each model. In either models, patients with low-risk scores had a better OS than those with high-risk scores ($p < 0.05$) (Figure 6a–f). Furthermore, we constructed an ROC curve to measure the performance of each model. The AUC of AT (0.793) was the highest among all models, while that of AD (0.624) was the lowest. The AUCs for RI, AP, ES, and AA were 0.729, 0.703, 0.786, and 0.652, respectively (Figure 6g).

3.7 Correlation between m6A methylation-related DEAS and BLCA prognosis in the validation dataset

Based on GSE13507, we validated that the prognosis of patients in the high-risk score group was significantly worse than that in the low-risk score group in all six

Table 1: TOP10 genes and corresponding alternative splicing events in protein–protein interaction network

Name	as_id	Betweenness	Closeness	Degree	Splice_type
AKT1	29559	935.6667	0.032219	9	AP
SRSF6	59434	102.6048	0.031733	9	ES
SRSF2	43660	228.1071	0.031911	9	RI
HNRNPA1	22149	264.0103	0.031923	8	ES
NUP62	51123	535.3992	0.032116	7	RI
HNRNPA2B1	79038	13.77143	0.031484	7	AA
SRSF7	53279	23.4	0.031658	7	RI
MCM7	80881	470	0.031583	6	AP
HNRNPL	49699	0.333333	0.031471	6	ES
HNRNPDL	69705	0.333333	0.031471	6	ES

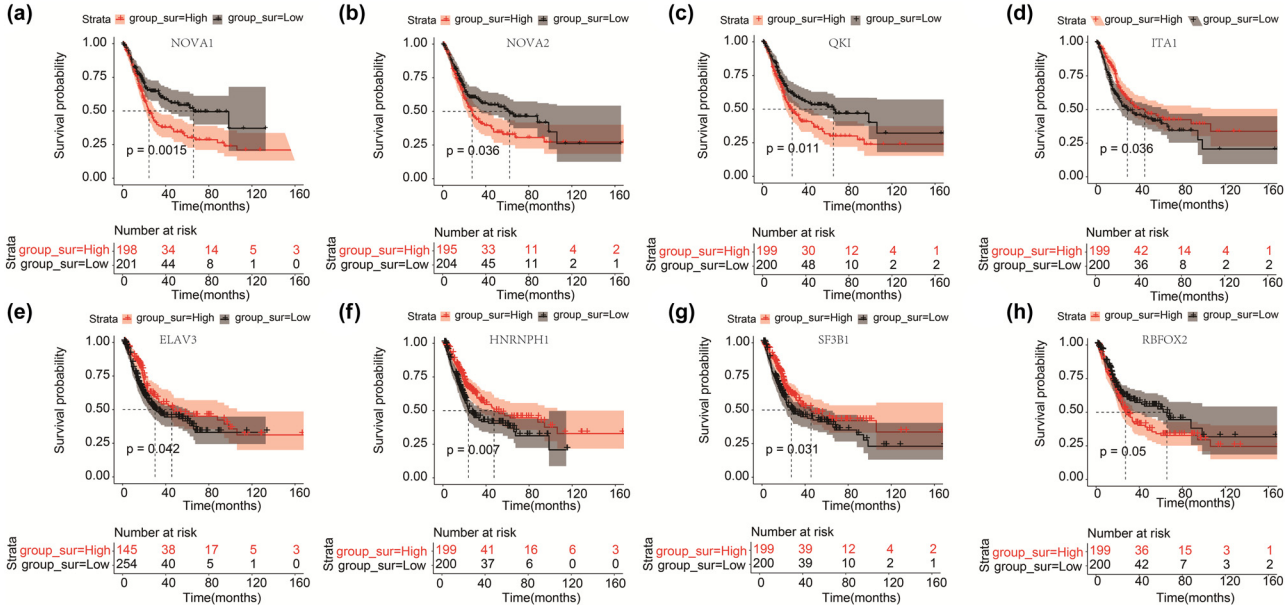

Figure 4: KM curves of the OS difference between high and low expression of SF. (a–h) Represent the KM curves of the OS difference between the high and low expression of NOVA1, NOVA2, QKI, ITA1, ELVA3, HNRNPH1, SF3B1, and RBFOX2, respectively.

models (AA, AD, AP, AT, ES, and RI) (Figure 7a–f). Further ROC analysis showed that all six models had good predictive performances. The AUCs for RI, AP, AT, AA, ES, and AD were 0.845, 0.809, 0.759, 0.738, 0.677, and 0.672, respectively (Figure 7g).

3.8 Screening of independent prognostic clinical factors

After performing a univariate Cox analysis, we found that TNM stage, age, and risk score were significantly associated

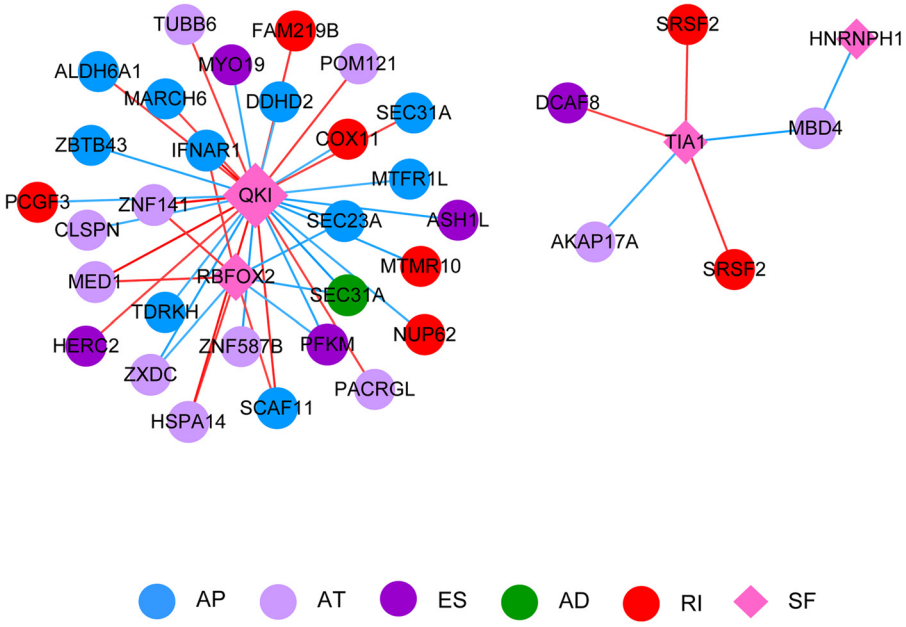

Figure 5: Correlation network between SF and the genes corresponding to AS events. Blue, lavender, purple, green, and red nodes represent AP, AT, ES, AD, and RI events, respectively. The pink diamond represents SF. AD, AP, AT, ES, RI. The red line indicates a positive correlation, and the blue line indicates a negative correlation.

with prognosis (data not shown, $p < 0.05$). Further multivariate Cox analysis showed that in the AS groups, except for AP ($p = 0.148$), the risk score was an independent prognostic factor of BLCA ($p < 0.05$) (Figure 8).

4 Discussion

BLCA is a common disease of the urinary system involving malignant tumors with a 60–70% recurrence rate after therapy [23]. Genetic factors, including AS, have been proved by many studies to play a role in the metastasis and development of BLCA [24]. m6A methylation modification is a potential target for cancer therapy and has been extensively studied in recent years [25]. However, there are few reports on combining m6A methylation modification and AS to analyze its role in BLCA species. The main purpose of this study was to explore whether the combined analysis of m6A methylation modification and AS will provide new insights into understanding the mechanism of BLCA.

We found that six AS types were significantly associated with OS. A significant correlation was also observed between m6A methylation regulators and AS events. In another study, m6A methylation regulators were found to play an important regulatory role in gene AS events [26]. Future studies will investigate the possible function of prognostic-related DEAS. Enrichment analysis revealed that they were mainly involved in RNA splicing regulation, cell cycle G2/M regulation, the MAPK signaling pathway, and prostaglandin response. These functions have been associated with various cancers [27]. Prostaglandins are lipids derived from polyunsaturated fatty acids. Recent studies suggest that it also plays a role in BLCA. Prostaglandin E2 (PGE2) is a highly expressed prostaglandin that controls a variety of normal, tissue-dependent physiological processes [28]. PGE2 has a tumor-promoting effect. It blocks cell death, enhances angiogenesis, promotes tumor inflammation, and prevents proper immune surveillance of tumors [29]. PGE2 shifts the phenotype of macrophages from antitumor M1 macrophages to pro-tumor M2 macrophages. PGE2/EP4 signaling can regulate macrophage plasticity [30]. Cyclooxygenase (COX)-2, one of the key

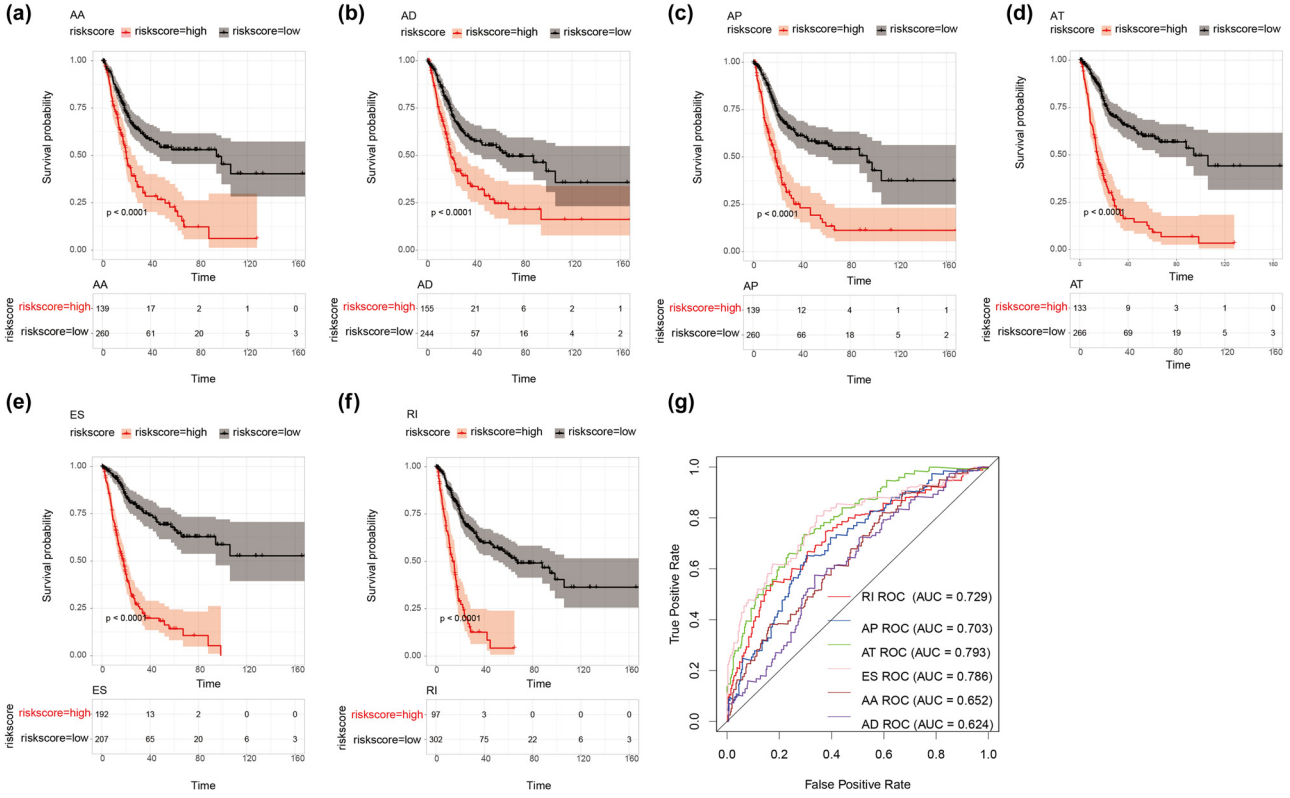

Figure 6: KM and ROC of prognostic predictors in the TCGA. (a–f) Represent the KM plot depicting the survival probability over time for the prognostic predictor of six types of AS events with the high- (red) and low- (blue) risk groups, respectively. (g) ROC analysis for all prognostic predictors.

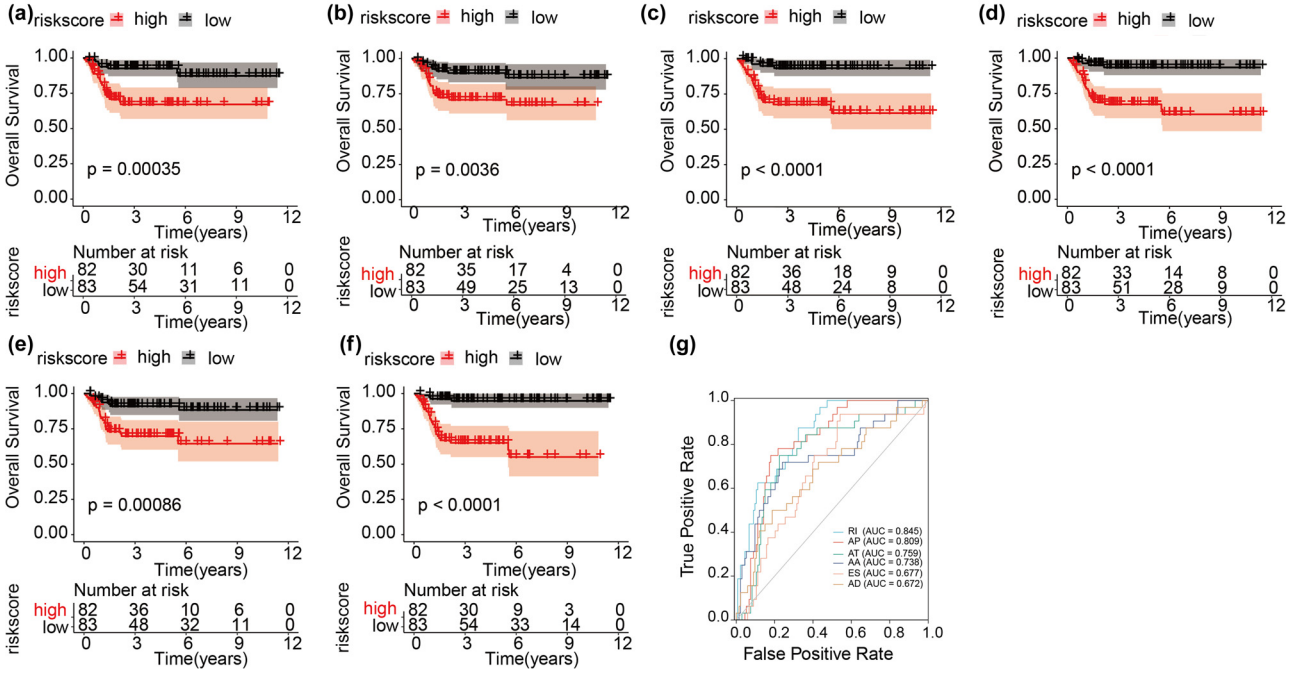

Figure 7: KM and ROC of prognostic predictors in GEO. (a–f) Represent the KM plot depicting the survival probability over time for the prognostic predictor of six types of AS events with the high- (red) and low- (blue) risk groups, respectively. (g) ROC analysis for all prognostic predictors.

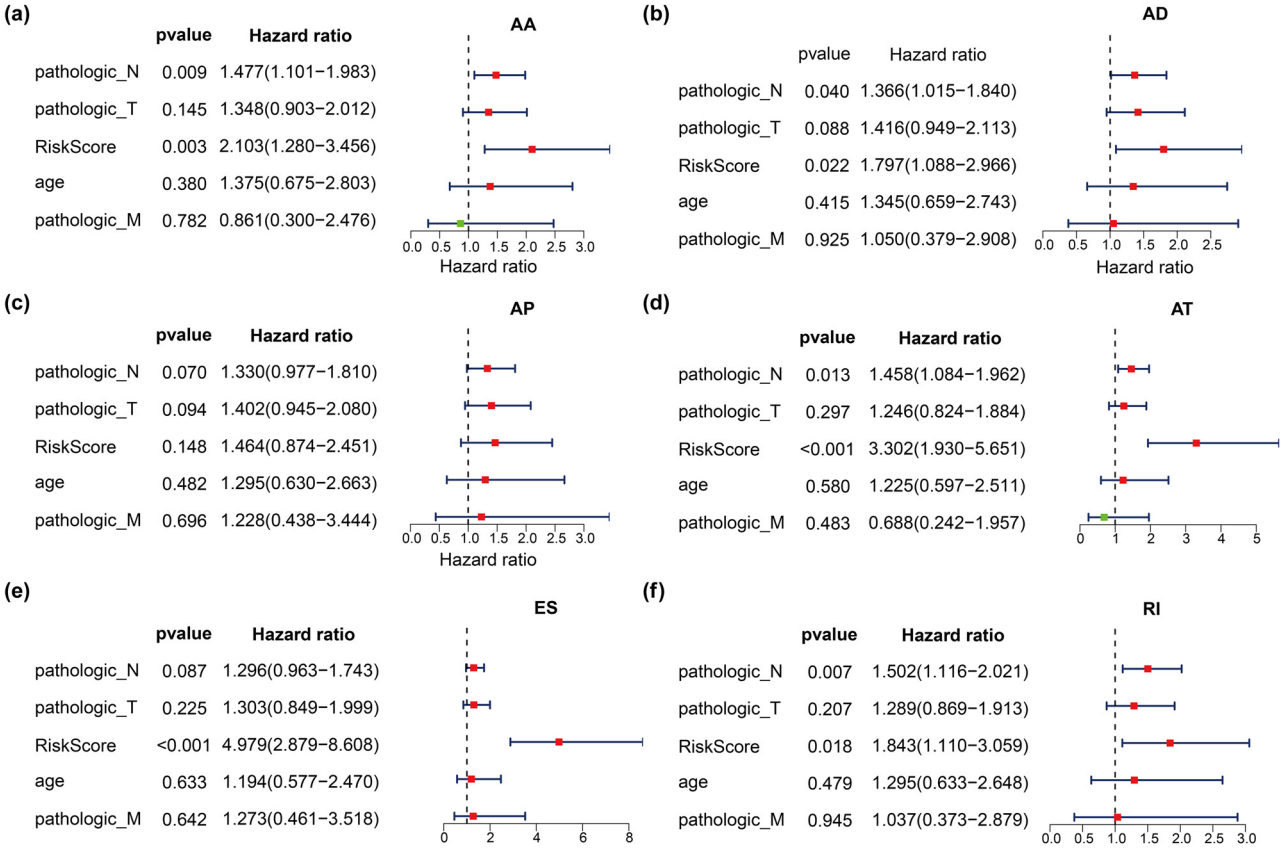

Figure 8: Forest plots for independent prognostic clinical factors based on multivariate Cox regression analysis. (a–g) Represent Forest plots for independent prognostic clinical factors in AA, AD, AP, AT, ES, and RI, respectively. AA and AD sites, AP, AT, ES, RI.

proteins responsible for angiogenesis and tumorigenesis, is highly expressed in BLCA. Prostaglandin levels were positively correlated with COX2 expression and BLCA progression [31]. Inhibition of COX enzymes by non-vehicle anti-inflammatory drugs results in decreased prostaglandin D2 levels, ultimately reducing the occurrence of BLCA [32].

There was an interaction relationship between the genes corresponding to the prognosis-related DEAS, and a PPI network consisting of 81 points was formed. The top three nodes in the network are AKT1, SRSF6, and SRSF2. TIA1 is an important tumor suppressor gene involved in many aspects of cancer occurrence and development and is considered a new tumor suppressor [33]. It regulates the expression of various mRNAs involved in proliferation, apoptosis, and angiogenesis of cancer cells [34]. TIA1 regulates RAB40B to inhibit cell proliferation [35]. In addition, TIA1 can promote apoptosis by regulating Fas AS [36]. SRSF6 and SRSF2 are serine/arginine-rich SFs. SRSF6 is essential for normal growth and development. SRSF6 also protects the genome from the formation of DNA–RNA hybrids (R-loops) following transcription [37]. Mutations in SRSF2 are associated with many diseases [38].

In addition, these prognosis-related DEAS interacted with SFs. Most poor prognostic AS events were inversely associated with SF expression, consistent with previous findings [39]. Upregulated expression of oncogenic SFs increases the oncogenic potential of protein variants and promotes cancer development [40]. These regulatory axes provide important guidance for subsequent exploration of the specific functional mechanisms of DEAS events.

We constructed six Cox proportional hazards regression models for the six OS-related AS types. An ROC curve was developed to evaluate the predictive efficiency of these models. The results revealed that the AUC of the AT model (0.793) was the highest, followed by ES (0.786), RI (0.729), AA (0.652), and AD (0.624). The above results show that our model has good predictive efficiency. Similarly, we also demonstrated the good predictive performance of the model in the GEO validation cohort. There has been no research on constructing a BLCA prognostic risk model using different AS types. Interestingly, AT showed the best predictive performance in the different types of AS-based prognostic risk models constructed for other cancers, such as glioma (AUC = 0.907) [41]. In another study on head and neck cancer, AT events were the most powerful prognostic factor [42].

Independence analysis revealed that the prognostic risk model based on multiple AS types was an independent prognostic factor for BLCA. A recent study demonstrated that high-throughput sequencing analysis is a key technique for characterizing the most common genetic aberrations in spliceosomes and splice sites [43]. In the future, clinical factors independent of age and TNM stage will be used to predict the prognosis of BLCA, and a combination of multiple clinical factors may yield better results.

This study had certain limitations. First, it was a retrospective study based on public databases. In the future, multiple centers, large samples, and more clinical features are needed to verify the results of this study. Second, BLCA is also affected by external environmental factors, such as smoking, in addition to genetic factors. Therefore, the constructed model needs further stratified verification. Third, whether the AS events obtained in our research actually exist still requires further experimental verification.

In conclusion, this study screened for prognostic-related AS events based on m6A methylation modification and constructed a reliable prognostic risk model. Further research on upstream SF predicted a possible regulatory relationship between SF and DEAS. This study provides insights for the subsequent understanding of the role of AS events in BLCA.

Funding information: This study was supported by the 12th Five-Year Social Science Research Project of the Jilin Provincial Education Department (No. 104115023).

Author contributions: Yuan Chang and Shukun Yu conceived and designed the study, and Miao Zhang and Tianshu Jiang participated in acquiring the data. Yuan Chang performed the analysis and interpretation of the data. Yuan Liu and Xiuyun Zhu designed the study and performed statistical analysis. Shukun Yu participated in obtaining funding. Yuan Chang and Shukun Yu conceived the study, participated in its design and coordination, helped draft the article, and revised the manuscript for important intellectual content. All authors have read and approved the final manuscript.

Conflict of interest: Authors state no conflict of interest.

Data availability statement: The datasets generated during and/or analyzed during the current study are available from the corresponding author on reasonable request.

References

[1] Xu Y, Wu G, Li J, Li J, Ruan N, Ma L, et al. Screening and identification of key biomarkers for bladder cancer: A study based on TCGA and GEO data. BioMed Res Int. 2020;2020:1–20.

[2] Ramirez D, Gupta A, Canter D, Harrow B, Dobbs RW, Kucherov V, et al. Microscopic haematuria at time of diagnosis is associated with lower disease stage in patients with newly diagnosed bladder cancer. BJU Int. 2016;117(5):783–6.
[3] Sanli O, Dobruch J, Knowles MA, Burger M, Alemozaffar M, Nielsen ME, et al. Bladder cancer. Nat Rev Dis Primers. 2017;3(1):1–19.
[4] Pelly VS, Moeini A, Roelofsen LM, Bonavita E, Bell CR, Hutton C, et al. Anti-inflammatory drugs remodel the tumor immune environment to enhance immune checkpoint blockade efficacy. Cancer Discovery. 2021;11(10):2602–19.
[5] Lopez-Beltran A, Cimadamore A, Blanca A, Massari F, Vau N, Scarpelli M, et al. Immune checkpoint inhibitors for the treatment of bladder cancer. Cancers. 2021;13(1):131.
[6] He L, Li H, Wu A, Peng Y, Shu G, Yin G. Functions of *N*6-methyladenosine and its role in cancer. Mol Cancer. 2019;18(1):1–15.
[7] Chen M, Nie Z-Y, Wen X-H, Gao Y-H, Cao H, Zhang S-F. m6A RNA methylation regulators can contribute to malignant progression and impact the prognosis of bladder cancer. Biosci Rep. 2019;39(12):BSR20192892.
[8] Tuncel G, Kalkan R. Importance of m N(6)-methyladenosine (m (6)A) RNA modification in cancer. Med Oncol. 2019;36(4):36.
[9] Zhang C, Fu J, Zhou Y. A review in research progress concerning m6A methylation and immunoregulation. Front Immunol. 2019;10:922.
[10] Song Y, Xu Q, Wei Z, Zhen D, Su J, Chen K. Predict epitranscriptome targets and regulatory functions of N (6)-methyladenosine (m(6)A) writers and erasers. Evolut Bioinforma. 2019;15:1176934319871290.
[11] Li J, Rao B, Yang J, Liu L, Huang M, Liu X, et al. Dysregulated m6A-related regulators are associated with tumor metastasis and poor prognosis in osteosarcoma. Front Oncol. 2020;10:769.
[12] Han J, Wang JZ, Yang X, Yu H, Zhou R, Lu HC, et al. METTL3 promote tumor proliferation of bladder cancer by accelerating pri-miR221/222 maturation in m6A-dependent manner. Mol Cancer. 2019;18(1):110.
[13] Ying X, Jiang X, Zhang H, Liu B, Huang Y, Zhu X, et al. Programmable *N*6-methyladenosine modification of CDCP1 mRNA by RCas9-methyltransferase like 3 conjugates promotes bladder cancer development. Mol Cancer. 2020;19(1):169.
[14] Kim CJ, Isono T, Tambe Y, Chano T, Okabe H, Okada Y, et al. Role of alternative splicing of periostin in human bladder carcinogenesis. Int J Oncol. 2008;32(1):161–9.
[15] Xie R, Chen X, Cheng L, Huang M, Zhou Q, Zhang J, et al. NONO inhibits lymphatic metastasis of bladder cancer via alternative splicing of SETMAR. Mol Ther. 2021;29(1):291–307.
[16] Ryan M, Wong WC, Brown R, Akbani R, Su X, Broom B, et al. TCGASpliceSeq a compendium of alternative mRNA splicing in cancer. Nucleic Acids Res. 2016;44(D1):D1018–D22.
[17] Hayles J. The gene ontology resource: 20 years and still GOing strong. England: Nucleic Acid Research; 2019.
[18] Kanehisa M, Goto S. KEGG: Kyoto encyclopedia of genes and genomes. Nucleic Acids Res. 2000;28(1):27–30.
[19] Yu G, Wang LG, Han Y, He QY. clusterProfiler: An R package for comparing biological themes among gene clusters. Omics A J Integr Biol. 2012;16(5):284–7.
[20] Szklarczyk D, Franceschini A, Wyder S, Forslund K, Heller D, Huerta-Cepas J, et al. STRING v10: protein–protein interaction networks, integrated over the tree of life. Nucleic acids Res. 2015;43(D1):D447–52.
[21] Shannon P, Markiel A, Ozier O, Baliga NS, Wang JT, Ramage D, et al. Cytoscape: A software environment for integrated models of biomolecular interaction networks. Genome Res. 2003;13(11):2498–504.
[22] Xiong Y, Deng Y, Wang K, Zhou H, Zheng X, Si L, et al. Profiles of alternative splicing in colorectal cancer and their clinical significance: A study based on large-scale sequencing data. EBioMedicine. 2018;36:183–95.
[23] Shariat SF, Sfakianos JP, Droller MJ, Karakiewicz PI, Meryn S, Bochner BH. The effect of age and gender on bladder cancer: A critical review of the literature. BJU Int. 2010;105(3):300.
[24] Guo Z, Zhu H, Xu W, Wang X, Liu H, Wu Y, et al. Alternative splicing related genetic variants contribute to bladder cancer risk. Mol Carcinog. 2020;59(8):923–9.
[25] Jiang X, Liu B, Nie Z, Duan L, Xiong Q, Jin Z, et al. The role of m6A modification in the biological functions and diseases. Signal Transduct Target Ther. 2021;6(1):1–16.
[26] Zhao Z, Cai Q, Zhang P, He B, Peng X, Tu G, et al. *N*6-Methyladenosine RNA methylation regulator-related alternative splicing (AS) gene signature predicts non–small cell lung cancer prognosis. Front Mol Biosci. 2021;8:486.
[27] Park C, Cha H-J, Lee H, Hwang-Bo H, Ji SY, Kim MY, et al. Induction of G2/M cell cycle arrest and apoptosis by genistein in human bladder cancer T24 cells through inhibition of the ROS-dependent PI3k/Akt signal transduction pathway. Antioxidants. 2019;8(9):327.
[28] Finetti F, Travelli C, Ercoli J, Colombo G, Buoso E, Trabalzini L. Prostaglandin E2 and cancer: Insight into tumor progression and immunity. Biology. 2020;9(12):434.
[29] Woolbright BL, Pilbeam CC, Taylor JA. Prostaglandin E2 as a therapeutic target in bladder cancer: From basic science to clinical trials. Prostaglandins Other Lipid Mediators. 2020;148:106409.
[30] Mizuno R, Kawada K, Sakai Y. Prostaglandin E2/EP signaling in the tumor microenvironment of colorectal cancer. Int J Mol Sci. 2019;20(24):6254.
[31] Bourn J, Cekanova M. Cyclooxygenase inhibitors potentiate receptor tyrosine kinase therapies in bladder cancer cells *in vitro*. Drug Des Dev Ther. 2018;12:1727–42.
[32] Jara-Gutiérrez Á, Baladrón V. The role of prostaglandins in different types of cancer. Cells. 2021;10(6):1487.
[33] Sánchez-Jiménez C, Izquierdo JM. T-cell intracellular antigens in health and disease. Cell Cycle. 2015;14(13):2033–43.
[34] Hamdollah Zadeh MA, Amin EM, Hoareau-Aveilla C, Domingo E, Symonds KE, Ye X, et al. Alternative splicing of TIA–1 in human colon cancer regulates VEGF isoform expression, angiogenesis, tumour growth and bevacizumab resistance. Mol Oncol. 2015;9(1):167–78.
[35] Reyes R, Alcalde J, Izquierdo JM. Depletion of T-cell intracellular antigen proteins promotes cell proliferation. Genome Biol. 2009;10(8):R87.
[36] Izquierdo JM, Majós N, Bonnal S, Martínez C, Castelo R, Guigó R, et al. Regulation of Fas alternative splicing by antagonistic effects of TIA-1 and PTB on exon definition. Mol Cell. 2005;19(4):475–84.
[37] Juge F, Fernando C, Fic W, Tazi J. The SR protein B52/SRp55 is required for DNA topoisomerase I recruitment to chromatin, mRNA release and transcription shutdown. PLoS Genet. 2010;6(9):e1001124.

[38] Rahman MA, Lin KT, Bradley RK, Abdel-Wahab O, Krainer AR. Recurrent SRSF2 mutations in MDS affect both splicing and NMD. Genes Dev. 2020;34(5–6):413–27.
[39] Zong Z, Li H, Yi C, Ying H, Zhu Z, Wang H. Genome-wide profiling of prognostic alternative splicing signature in colorectal cancer. Front Oncol. 2018;8:1–9.
[40] Wan L, Yu W, Shen E, Sun W, Liu Y, Kong J, et al. SRSF6-regulated alternative splicing that promotes tumour progression offers a therapy target for colorectal cancer. Gut. 2019;68(1):118–29.
[41] Xie ZC, Wu HY, Dang YW, Chen G. Role of alternative splicing signatures in the prognosis of glioblastoma. Cancer Med. 2019;8(18):7623–36.
[42] Liang Y, Song J, He D, Xia Y, Wu Y, Yin X, et al. Systematic analysis of survival-associated alternative splicing signatures uncovers prognostic predictors for head and neck cancer. J Cell Physiol. 2019;234(9):15836–46.
[43] Casamassimi A, Federico A, Rienzo M, Esposito S, Ciccodicola A. Transcriptome profiling in human diseases: New advances and perspectives. Int J Mol Sci. 2017;18(8):1652.